2016 23rd International Conference on Pattern Recognition (ICPR)
Cancún Center, Cancún, México, December 4-8, 2016

Detection of Glare in Night Photography

Mandakinee Singh, Rajesh Kumar Tiwari,
Kunal Swami, Ajay Vijayvargiya
Samsung R&D Institute India - Bangalore
Bangalore, India
Email: {mandakinee.p, rajesh.k.t, kunal.swami, ajay.v}@samsung.com

***Abstract*—Glare is a hardware problem that occurs because of the light trapped in the lens elements. It is a common problem faced in photography when trying to capture image of a scene having bright source in it or taken in a very bright environment. Glare can hide useful information in the image, can make foreground objects blurry and deformed. In this paper, we propose a novel method to detect glare, mainly focusing on scenario where users take photo of scene having light source in outdoor environment during night. The method described in the paper takes combination of three different masks of original image to detect the glare. First mask is obtained by image segmentation of original image using our improved Bernsen's local thresholding method. To obtain second mask, we binarize the original image by simple thresholding to get specular hot-spot of light present in the original image and for the third mask, we apply thresholding on each RGB channel of original image. Finally, glare is detected using connected component computation on aforementioned masks. The proposed solution detects the glare affected area with very good accuracy.**

***Index Terms*—Glare, Bernsen's Local Thresholding Method, Connected Component, Specular Hotspot, Smearing, Blooming, Binarization**

I. Introduction

Glare is characterized as a physical defect of lens. The reflective surfaces of lens cause the light to bounce back and forth between its lens elements. In cameras where the flange distance (distance of first element of the lens sequence from imaging sensor) is very small, like in mobile/tablet cameras and mirror-less cameras, light is first squeezed into a very small aperture and then reflected multiple times between the lens sequences as shown in fig. 1. This results into amplification of intensity of the neighboring pixels of light source in the image. In case of light sources like sun, pixels throughout the image gets intensified and intensity value of pixels gradually decreases as the distance from the source increases. Specifically, the bright regions which were supposed to constitute few pixels in the image get enlarged and form a spread of decreasing intensity. When image of a very bright source, unlike sun, is taken in dark environment, this effect is more profound as intensity of pixels corresponding to the light source regions are amplified and the bright region spreads to the neighboring areas giving glare to the image. So, while capturing bright light sources, the source of light appears as a bright white sphere with straight lines running through the sphere. The bright sphere is called blooming glare and the straight lines are called smearing glare as shown in fig. 2.

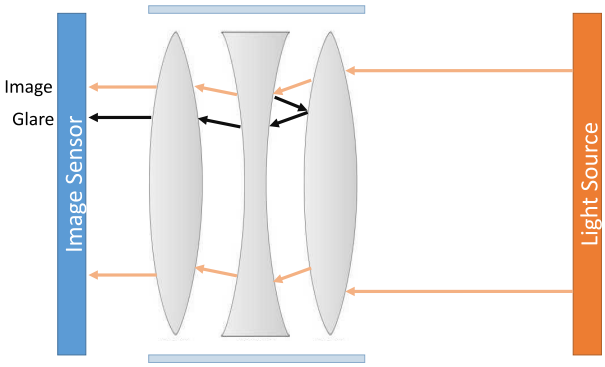

Fig. 1. Glare Phenomenon

Glare is camera's hardware drawback and can be rectified if either the camera is equipped with anti-glare lens or some other filter like polarization filter is applied physically to remove the glare in pre-processing stage (i.e., before the image is taken). Previous attempts in glare removal address the problem at hardware level by use of anti-glare coatings [1]. To achieve the same goal using software, first the glare area needs to be identified. Since, glare is prominently formed around bright objects and its effect is local, a locally adaptive thresholding is to be adopted which can distinguish regions based on contrast value in local region [2], [3] like the ones proposed by White and Rohrer [4], Bernsen [5] and Yasuda et al. [6]. We have modified the original Bernsen's local thresholding method [5] and used it to determine a local

(a) (b)

Fig. 2. Glare in night environment: (a) Blooming Glare (b) Smearing Glare

contrast based threshold in order to distinguish foreground and background. But this alone is not sufficient, so additional masks are required to detect glare accurately.

When an image is taken in outdoor environment at night, due to the presence of light source in field of view, blooming and smearing glare can occur in camera preview or snapshot. This glare can alter the important information present in both background and foreground. In this paper, we are mainly focusing to detect smearing and blooming glare in outdoor images having bright light sources at night. This solution can be easily integrated in the existing mobile and camera platforms without any hardware modification. Detecting and removing glare can have striking advantages in night photography. The major contribution of the paper is:

A novel method to detect the glare affected region using our new improved Bernsen's local thresholding method explained in section III-A and multiple thresholding mask defined in section III.

A. *Literature Review*

Most of the existing literature recognize the glare present on objects and remove it based on either the immediate environment/neighboring area or the overall intensity distribution in the image. In some cases, the camera preview with extra exposure to the bright environment is filtered based on the overall image intensity and exposure. In general, papers refer to removal of the glare of objects due to light source.

In [8], a different type of glare, veiling glare , which is caused by the presence of light source in field of view or near to field of view has been addressed. The thickness of such glare is very less, so it is assumed to be noise and a deconvolution filter is applied to mask it out. But in case of significant glare, glare removal using deconvolution gives poor results; so structured occlusion mask method is applied in [9] before image acquisition. However, this might increase the image acquisition time by a significant amount.

In [10], the image is divided into two parts, saturated and unsaturated pixels. Glare formation from these pixels is different and hence solved separately.

In the paper [7], light distribution by the bright source is modeled by constructing a multi-layered structure using distance transform. First bilateral filter is applied to separate the layers in original image. Based on a threshold value on the hue channel of the original image, the locations of light source are identified, pixels are labeled and similar layers are grouped based on distance transform. Using this similarity, glare region is detected.

II. METHODOLOGY

To remove glare, an understanding of the behavior of light with the lens elements is required. In this section we explain our approach and algorithm.

1	0	1	1	1	1	0	0
1	0	1	0	1	1	1	0
1	0	0	1	1	0	1	1
1	0	0	0	1	0	1	1
0	0	0	0	0	0	1	0
0	0	0	0	0	0	0	0
0	0	0	0	0	0	0	0
0	0	0	0	0	0	0	0

(a)

1	0	2	2	2	2	0	0
1	0	2	0	2	2	2	0
1	0	0	2	2	0	2	2
1	0	0	0	2	0	2	2
0	0	0	0	0	0	2	0
0	0	0	0	0	0	0	0
0	0	0	0	0	0	0	0
0	0	0	0	0	0	0	0

(b)

Fig. 3. (a) Connected Components (b) Labeled Components

The proposed method is based on the intensity variation of the glare affected region and regions connected to light source. Before we explain our algorithm, we explain the intensity variation of smearing and blooming glare and the connected component method. In most images, the point light sources have highest intensity in the whole image. The intensity of blooming glare present in surrounding of the light source decreases as we move away from the light source. Smearing glare are bright straight lines which pass through the light source and have higher intensity at center which decreases as we move towards the ends of the smear line and its boundaries. To find the region of the glare we need to detect the regions or components connected to the light source. Connected component is a method to find a set of pixels that form a connected group which are then labeled together as shown in fig. 3. It is a popular way to segment a binary image by clubbing similar neighboring pixels together. The components are labeled and the pixels of same component share the same number.

In our proposed solution, we start with the original image and perform different image binarization methods to get different masks. Image binarization is a technique to segment image into connected group of pixels. Fig. 4 shows steps of proposed algorithm and fig. 5 shows the intermediate masks of a sample input. We prepare the first mask $\mathcal{M}$ using Bernsen's local thresholding (section III-A) binarization method. This method segments the image into foreground and background (refer to section III-B for detailed explanation). Second mask $\mathcal{N}$ is obtained by taking higher intensities in the image. To isolate the glare region from the foreground of this mask, maximum connected components of the $\mathcal{M}$ with $\mathcal{N}$ is found and named as $\mathcal{P}$, similarly maximum connected component of $\mathcal{N}$ with $\mathcal{P}$ is found and named it $\mathcal{Q}$. To get the proper spread of blooming and width of smearing glare, one more mask $\mathcal{R}$ is made by finding the pixels in image having grayscale property (in ideal case, the sum of absolute differences between R, G and B is assumed zero) and applying a threshold on these pixels on each RGB channel. To remove the artifacts from $\mathcal{R}$, connected components of $\mathcal{R}$ with $\mathcal{Q}$ is computed to get another mask $\mathcal{S}$. To get the final detection mask we fuse $\mathcal{S}$ with $\mathcal{P}$. Based on the solution requirement, the threshold values should

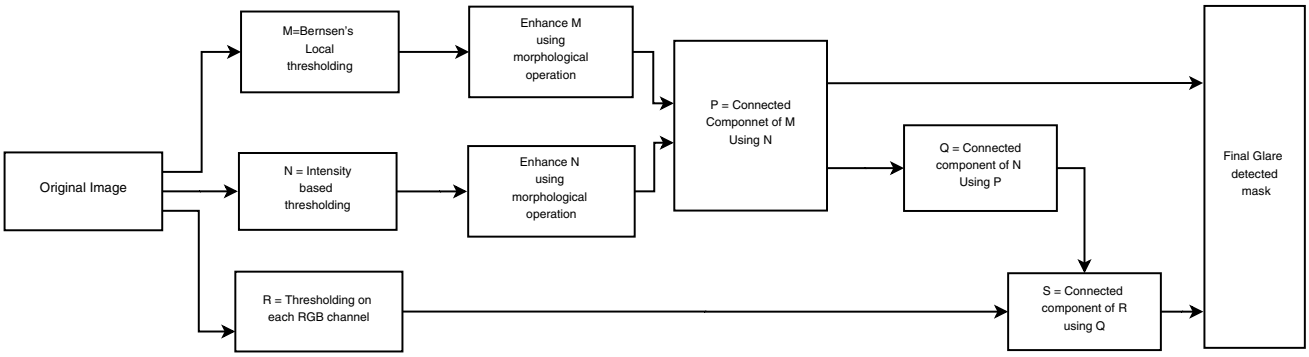

Fig. 4. Method proposed in the paper to detect glare

be chosen for the image binarization. High value of threshold can lead to incomplete detection and low value can lead to introduction of many false artifacts.

This paper presents a method to detect glare using a new improved version of Bernsen's local thresholding algorithm defined in the section III-A.

A. *Bernsen's Local Thresholding*

The Bernsen's local thresholding algorithm is widely used algorithm for local thresholding. Bernsen's local thresholding method calculates the minimum, maximum intensity pixel and the mean of pixels in the neighborhood of each pixel for given window size.

Let $\mathcal{I}(i,j)$, $\mathcal{I}_{max}(i,j)$, $\mathcal{I}_{min}(i,j)$, $c(i,j)$, $g(i,j)$ and $b(i,j)$ be the gray value, maximum gray value, minimum gray value, local contrast value, median value and Bernsen's local thresholding value respectively for pixel present at (i,j) for window size of $N \times N$.

$$g(i,j) = \frac{\mathcal{I}_{max}(i,j) + \mathcal{I}_{min}(i,j)}{2} \tag{1}$$

$$c(i,j) = \mathcal{I}_{max}(i,j) - \mathcal{I}_{min}(i,j) \tag{2}$$

$$b(i,j) = \begin{cases} 1, & \text{if } (\mathcal{I}(i,j) < \mathcal{I}^* \ AND \ c(i,j) < c^*) \\ & OR \ (\mathcal{I}(i,j) < g(i,j) \ AND \ c(i,j) \geq c^*) \\ 0, & \text{otherwise.} \end{cases} \tag{3}$$

Where c^* and $\mathcal{I}^*$ are contrast threshold and gray value threshold respectively.

III. Proposed Method

We proposed a new improved Bernsen's local thresholding for segmentation of image which is explained in section III-A.

A. *Improved Bernsen's Local Thresholding*

In the proposed method, instead of just giving a constant value for intensity comparison in equation (3), mean of gray scale values has also been evaluated for each window to produce better results.

A window size of $N \times N$ is taken for each target pixel for the calculation of minimum, maximum and mean intensities. A threshold value of contrast is chosen after doing the appropriate observation on the dataset.

Let $\mu(i,j)$ be the mean value for pixel present at (i,j) for window size of $N \times N$.

$$c(i,j) = \mathcal{I}_{max}(i,j) - \mathcal{I}_{min}(i,j) \tag{4}$$

$$\mu(i,j) = \sum_{m=-N/2}^{N/2} \sum_{n=-N/2}^{N/2} \frac{\mathcal{I}(i+m, j+n)}{N \times N} \tag{5}$$

$$b^*(i,j) = \begin{cases} 1, & \text{if}((\mathcal{I}(i,j) \geq \mu(i,j) \ AND \ (c(i,j) < c^*) \\ & OR \ (c(i,j) \geq c^* \ AND \ \mathcal{I}(i,j) \geq I_c))) \\ 0, & \text{otherwise.} \end{cases} \tag{6}$$

Where c^* and I_c are contrast threshold and threshold constant respectively. These constant values are chosen after experimenting on our dataset, whereas in original Bernsen's local thresholding method explained in section II-A, these values are determined by the Otsu's global thresholding method.

B. *Intermediate Masks*

As mentioned earlier, we are presenting a solution for glare detection using multiple masks; we will explain the formation of these masks in the following subsections:

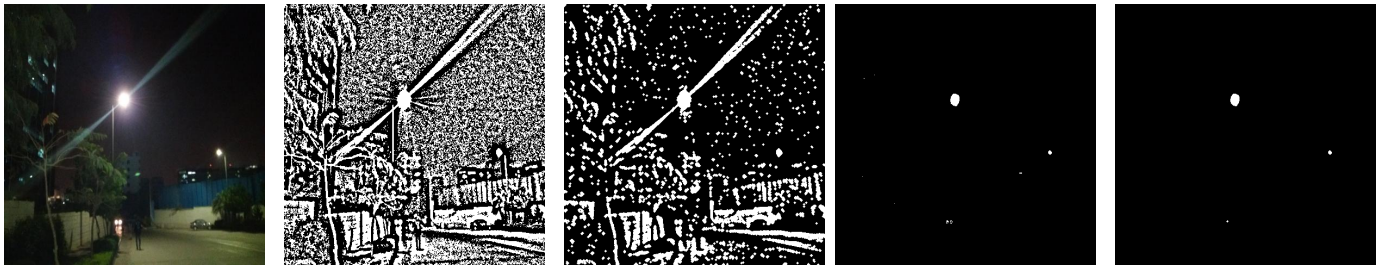

(a) Original image (b) Mask $\mathcal{M}$ (c) Mask $\mathcal{M}$ after Filtration (d) Mask $\mathcal{N}$ (e) Mask $\mathcal{N}$ after Filtration

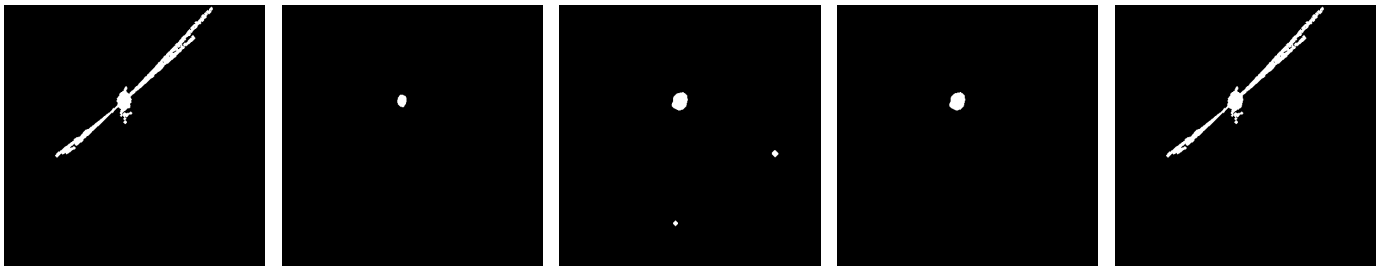

(f) mask $\mathcal{P}$ (g) Mask $\mathcal{Q}$ (h) Mask $\mathcal{R}$ (i) Mask $\mathcal{S}$ (j) Final Detection Mask

Fig. 5. Glare detection for an input image with all its intermediate masks

1) Construction of Intermediate Mask $\mathcal{M}$: We use the above defined method for first level of binarization (fig. 5b). To enhance this mask we apply morphological filtering on it (fig. 5c). The mask still contains many false positives which need to be processed further.

$$\mathcal{I}_{\mathcal{M}} = b^*(i,j) \tag{7}$$

2) Construction of Intermediate Mask $\mathcal{N}$: To isolate the regions affected by glare and remove the false detections, we first convert the original image (fig. 5a) to gray scale image and find highest gray value point $\mathcal{I}_{max}$ in this converted image and then we binarize the gray-scale image with thresholding factor 0.99 of $\mathcal{I}_{max}$ to get the hot-spot of light source in mask and we call this mask as $\mathcal{N}$ (fig. 5d). This mask needs further filtration to remove the false small white spots (fig. 5e).

$$\mathcal{I}_{\mathcal{N}}(i,j) = \begin{cases} 1 \text{ if } \mathcal{I}(i,j) > (\mathcal{I}_{max} \times 0.99) \\ 0 \text{ otherwise} \end{cases} \tag{8}$$

-

3) Construction of Intermediate Mask $\mathcal{P}$ and $\mathcal{Q}$: To remove the false detection from the mask, we use connected component method to find the maximum connected component present in mask $\mathcal{M}$ corresponding to the region present in mask $\mathcal{N}$ to get an intermediate mask $\mathcal{P}$ (fig. 5f). Now we will use this mask $\mathcal{P}$ to find the connected component present in mask $\mathcal{N}$ corresponding to regions present in mask $\mathcal{P}$ and get another intermediate mask $\mathcal{Q}$ (fig. 5g).

$$\mathcal{P} = \mathcal{M} \oplus \mathcal{N} \tag{9}$$

$$\mathcal{Q} = \mathcal{N} \oplus \mathcal{P} \tag{10}$$

Where $\oplus$ represents the operation for finding maximum connected component on first operand mask which has at least one common element with second operand.

4) Construction of Intermediate Mask $\mathcal{R}$ and $\mathcal{S}$: The processed mask $\mathcal{P}$ does not give the proper detection of spread of the smearing glare and blooming glare. To get the spread of the smear with its boundaries we first check gray scale property of each pixel i.e. the sum of absolute differences of the R, G and B values is approximately equal to zero. If the pixel satisfies the property and either of the RGB channel have pixel value greater than a threshold value, we consider this pixel as foreground. But again this intermediate mask may contain many false positives which lead us to do further filtration on it to get the additive mask $\mathcal{R}$ (fig. 5h).

Let $\mathcal{I}_R(i,j)$, $\mathcal{I}_G(i,j)$, $\mathcal{I}_B(i,j)$ and $\mathcal{R}(i,j)$ be the red channel, green channel, blue channel and mask $\mathcal{R}$ pixel value at (i,j).

$$\mathcal{R} = \begin{cases} 1, & \text{if}((|(\mathcal{I}_R - \mathcal{I}_G)| + |(\mathcal{I}_G - \mathcal{I}_B)| + |(\mathcal{I}_B - \mathcal{I}_R)| < C) \\ & \quad AND\ ((\mathcal{I}_R > 0.8 \times (\mathcal{I}_R)_{max}) \\ & \quad OR\ (\mathcal{I}_G > 0.8 \times (\mathcal{I}_G)_{max}) \\ & \quad OR\ (\mathcal{I}_B > 0.8 \times (\mathcal{I}_B)_{max}))) \\ 0, & \text{otherwise.} \end{cases} \tag{11}$$

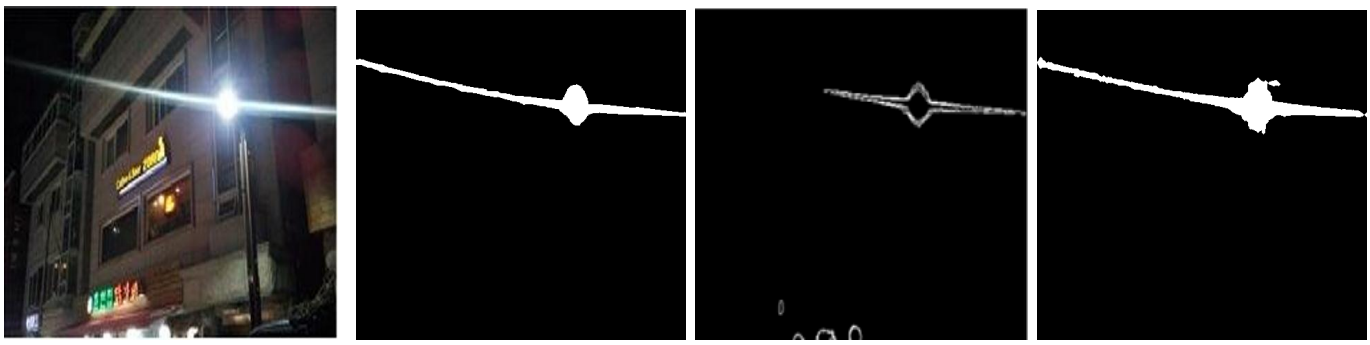

(a) (b) (c) (d)

Fig. 6. In the above figures (a) shows Source image, (b) shows the ground truth image, (c) Glare detection in [7] and (d) shows Glare detection using proposed method

Where C is a constant value to check gray scale property of the pixels which should be kept low (kept as 0 in ideal cases). We tested a range of values on our dataset and got an optimal value of 29 for C.

The mask $\mathcal{R}$ may contains many other large components which would have not been removed by filtration. We handle this by taking the maximum connected component present in mask $\mathcal{R}$ corresponding to the mask $\mathcal{Q}$. We call this mask as $\mathcal{S}$ (see fig. 5i).

$$\mathcal{S} = \mathcal{R} \oplus \mathcal{Q} \tag{12}$$

5) Construction of Final Detection Mask: Fuse the mask $\mathcal{S}$ with mask $\mathcal{P}$ to get the final detection of the glare as shown in fig. 5j.

$$\text{Final Detection} = \mathcal{S} \cup \mathcal{P} \tag{13}$$

IV. Experimental Results

In this section, we show the results achieved by the method presented in this paper. We compare our solution with the method proposed by [7]. (The fig. 6a and 6c is taken from [7] for comparison purpose.) If one observes carefully, the method in [7] does not detect the whole area of glare. It uses the multilayer technology through distance transformation which quantizes the image to make layers and these layers are combined when the fraction of overlapped region between two adjacent layers is beyond a threshold value. The layer size increases as we focus for the smear glare, hence, the above defined ratio fails to get the pixels in the trailing edge of the glare because it lies in the region not recognized by threshold. Whereas the method defined in this paper uses the new modified Bernsen's local thresholding method for first level of image binarization to properly segment the glare in the image. We tested a range of values for window size (N) and contrast threshold (c^*) on our dataset and we finally converged to the optimal values of 35 for contrast threshold (c^*) and 17x17 for window size (N).

In order to evaluate the proposed solution of this paper, we manually computed the ground truth for all the input images. We calculated Precision (P) and Recall (R) matrices for our method.

1) Precision and Recall: Precision (P) is the percentage of glare areas that are detected correctly in final mask.

Recall (R) is the percentage of the true glare area which was detected in final mask.

$$P = \frac{A_d \cap A_g}{A_d} \tag{14}$$

$$R = \frac{A_d \cap A_g}{A_g} \tag{15}$$

Where A_d denotes the area detected as glare and A_g denotes the ground truth glare area.

2) F-measure: F-measure is harmonic mean of precision and recall. We calculate the F-measure to evaluate the overall performance by taking the combination of both precision and recall. F-measure is calculated as follows:

$$F = \frac{2PR}{P+R} \tag{16}$$

In fig. 7, we have the detection mask and the ground truth for each input image. We calculated the precision, recall and F-measure using the above formulas and the results is shown in the following table I:

TABLE I
QUANTITATIVE EVALUATION OF OUR GLARE DETECTION METHOD

Precision	Recall	F-measure
0.7361	0.9207	0.8184

The proposed method is implemented in MATLAB®2013b on Linux with Intel® core™ i3-2120 CPU @ 3.30GHz x 4 processor with 4GB RAM . The time taken by the solution to detect glare for image size of 480×480 is 1.72s.

Figure 6 shows the subjective comparison between our method and [7]. From the results, one can easily derive that our method gives better detection results it also detects the trailing edge of the glare.

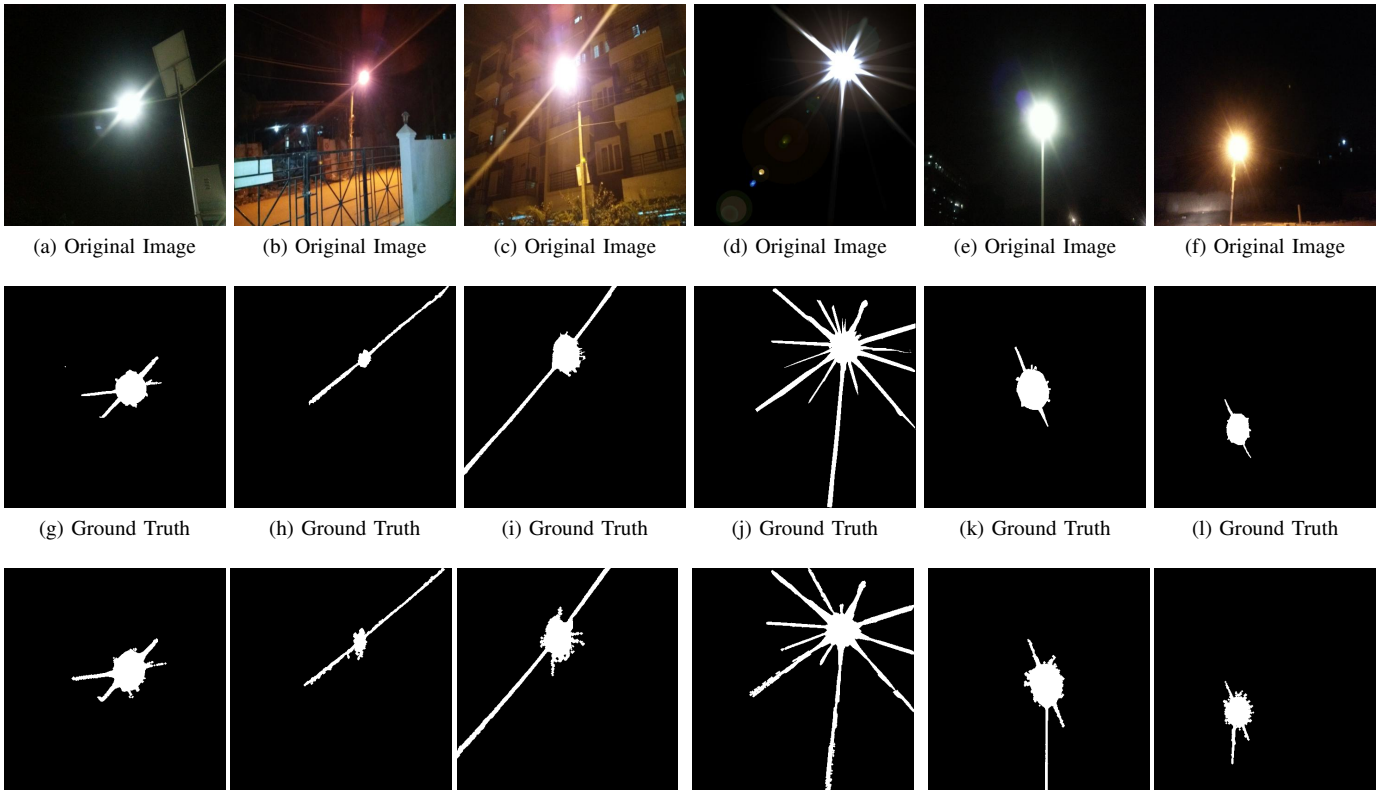

(a) Original Image (b) Original Image (c) Original Image (d) Original Image (e) Original Image (f) Original Image

(g) Ground Truth (h) Ground Truth (i) Ground Truth (j) Ground Truth (k) Ground Truth (l) Ground Truth

(m) Final Detection Mask (n) Final Detection Mask (o) Final Detection Mask (p) Final Detection Mask (q) Final Detection Mask (r) Final Detection Mask

Fig. 7. Final detection masks and ground truth images of various input image. Original images are shown in first row, ground truth for the respective images is in second row and third row has the final detection mask

V. Conclusion and Future Work

In this paper we have defined a novel method to detect glare in photos taken in outdoor environment during night. Our method detects the entire glare region including its trailing edges as shown in the fig. 6d, 7m, 7n, 7o, 7p and 5j. Our proposed method may give false positives sometimes because of artifacts present in background as shown in fig. 7q and 7r. This happens because light spreads very fast on brighter and metal surfaces which can also be detected as a part of glare.

We compared our results with [7] and showed that the detection is quite proper with our method for fig. 6.

As future work, we will mold this solution to detect glare introduced by multiple light sources in image. We would like to extend the solution further to recover the areas affected by glare.

ACKNOWLEDGMENT

We are thankful to Dr. Venkat R. Peddigari, Mr. Bhaskar Bagchi, Mr. Sidakpreet Singh Chawla and all the anonymous reviewers for their invaluable time, feedback and suggestions.

References

[1] H. K. Raut, V. A. Ganesh, A. S. Nair, and S. Ramakrishna, "Anti-reflective coatings: A critical, in-depth review," *Energy & Environmental Science*, vol. 4, no. 10, pp. 3779–3804, 2011.

[2] M. Nandy and S. Saha, "An analytical study of different document image binarization methods," *arXiv preprint arXiv:1501.07862*, 2015.

[3] W. Bieniecki and S. Grabowski, "Multi-pass approach to adaptive thresholding based image segmentation," in *Proceedings of the 8th International IEEE Conference CADSM*, 2005, pp. 418–423.

[4] J. M. White and G. D. Rohrer, "Image thresholding for optical character recognition and other applications requiring character image extraction," *IBM Journal of Research and Development*, vol. 27, no. 4, pp. 400–411, July 1983.

[5] J. Bernsen, "Dynamic thresholding of grey-level images," in *International conference on pattern recognition*, 1986, pp. 1251–1255.

[6] Y. Yasuda, M. Dubois, and T. S. Huang, "Data compression for check processing machines," *Proceedings of the IEEE*, vol. 68, no. 7, pp. 874–885, July 1980.

[7] C.-S. Cho, J. Song, and J.-I. Park, "Glare region detection in night scene using multi-layering," in *The Third International Conference on Digital Information Processing and Communications*. The Society of Digital Information and Wireless Communication, 2013, pp. 467–469.

[8] J. Seibert, O. Nalcioglu, and W. Roeck, "Removal of image intensifier veiling glare by mathematical deconvolution techniques," *Medical physics*, vol. 12, no. 3, pp. 281–288, 1985.

[9] E.-V. Talvala, A. Adams, M. Horowitz, and M. Levoy, "Veiling glare in high dynamic range imaging," *ACM Trans. Graph.*, vol. 26, no. 3, Jul. 2007. [Online]. Available: http://doi.acm.org/10.1145/1276377.1276424

[10] M. Rouf, R. Mantiuk, W. Heidrich, M. Trentacoste, and C. Lau, "Glare encoding of high dynamic range images," in *Computer Vision and Pattern Recognition (CVPR), 2011 IEEE Conference on*, June 2011, pp. 289–296.

[11] "A threshold selection method from gray-level histograms," *IEEE Transactions on Systems, Man, and Cybernetics*, vol. 9, no. 1, pp. 62–66, Jan 1979.